

# Interactions in a transversely isotropic new modified couple stress thermoelastic thick circular plate with two temperature theory

Parveen Lata<sup>a</sup> and Harpreet Kaur\*

Department of Basic and Applied Sciences, Punjabi University, Patiala, Punjab, India

(Received January 16, 2023, Revised April 21, 2023, Accepted May 8, 2023)

**Abstract.** This article is an application of new modified couple stress thermoelasticity without energy dissipation in association with two-temperature theory. The upper and lower surfaces of the plate are subjected to an axisymmetric heat supply. The solution is found by using Laplace and Hankel transform techniques. The analytical expressions of displacement components, conductive temperature, stress components and couple stress are computed in transformed domain. Numerical inversion technique has been applied to obtain the results in the physical domain. Numerically simulated results are depicted graphically. The effect of two temperature is shown on the various components.

**Keywords:** concentrated and distributed source; Hankel transform; Laplace transform; new modified couple stress; thermoelastic; transversely isotropic

---

## 1. Introduction

Classical continuum theory was not able to predict the size effects at nano/micro scale. So, Higher order theories came into the existence. A couple stress theory is an extended continuum theory that comprises the effects of couple stresses on a material volume, in addition to the classical normal and shear forces per unit area. This immediately admits the possibility of asymmetric stress tensor. The two additional constants are related to the underlying microstructure of the material and are inherently difficult to determine (e.g., Lakes 1982, Lam *et al.* 2003). Hence, there has been a need to develop higher-order theories involving only one additional material length scale parameter. The modified couple-stress theory was developed by Yang *et al.* (2002) that contains only one material length scale parameter. Modified couple stress theory was not applicable to anisotropic materials. So, Chen and Si (2013) developed a model of composite laminated beam on the basis of the global-local theory and new modified couple-stress theory for anisotropic elasticity.

Li *et al.* (2013) extended the modified couple stress theory in the isotropic elasticity to

---

\*Corresponding author, Ph.D. Scholar, E-mail: mehrokpreet93@gmail.com

<sup>a</sup>Associate Professor, E-mail: parveenlata@pbi.ac.in

anisotropic composite laminated plate. Buckling analysis of plate is done by simplifying the model to one material length constant. Chen and Li (2013) analysed micro-scale free vibration of composite laminated Timoshenko beam (CLTB) based on the new modified couple stress theory. In this theory, a new anisotropic constitutive relation is defined for modeling the CLTB. This theory uses rotation-displacement as dependent variable and contains only one material length scale parameter. Chen and Li (2014) proposed the new modified couple stress theory (NM-CST) for anisotropic materials containing three length scale parameters. Yang and Chen (2015) proposed the models of composite laminated micro-plates using a series of assumptions of new modified couple stress theory. Chen and Wang (2016) developed a composite laminated Reddy plate model based on the global-local theory and new modified couple-stress theory. There is only one micro material length scale constant in each layer of the composite laminated plate. This model fulfills the free surface condition, the geometric and stresses continuity conditions at interfaces. He *et al.* (2017) studied a size-dependent composite laminated skew Mindlin plate model based on a new modified couple stress theory and principle of minimum potential energy. Yang and He (2017) proposed a microstructure-dependent orthotropic functionally graded micro-plate model for the free vibration and buckling analysis based on the re-modified couple stress theory and principle of minimum potential energy. The macro- and microscopic anisotropy are simultaneously taken into account. Zihao and He (2019) studied the bending of orthotropic functionally graded micro-plates on the basis of a re-modified couple stress theory. The proposed model considered the micro- as well as macroscopic anisotropy of the plate. Yang and He (2019) proposed a orthotropic microstructure-dependent plate model for bending of functionally graded micro-plates using re-modified couple stress theory. Chen *et al.* (2019) studied the flapwise vibration of rotating composite microbeam with geometrical imperfection by combining isogeometric analysis and a re-modified couple stress theory (RMCST) for anisotropic elasticity. The effect of angular velocity, slender ratio, scale parameter, maximum imperfection amplitude, and ply angle on the flapwise vibration of rotation composite microbeam is investigated. Using re-modified couple stress theory and the Refined Zigzag theory, Yang and He (2019) examined the vibration and buckling of functionally graded (FG) sandwich micro-plates embedding functionally graded layers. Free vibrations and buckling of orthotropic microplates is examined by Mazur *et al.* (2020) based on the modified couple stress theory and Kirchhoff-Love plate theory. The influence of the material length scale parameter, boundary conditions, shape parameters, material characteristics on vibration frequencies is investigated. Zhou *et al.* (2022) developed a model of transversely isotropic piezoelectric bilayered rectangular micro-plate with a distributed load based on the couple stress piezoelectric theory. Zhang *et al.* (2022) studied the free vibration, buckling and post-buckling behaviors of bidirectional functionally graded (BDFG) microbeams employing the Timoshenko beam theory and the consistent couple stress theory (C-CST). The material properties of a BDFG microbeam were varied continuously in both thickness and axial directions. A model of thermal scale effect was proposed by Si *et al.* (2022), based on new modified couple stress theory, for the laminated composite plates of enhanced Reddy theory. Numerical results show that as the material length parameter increases, the scale effects of plates are enhanced. Also, the scale effects are weakened with increasing of span-thickness ratio of plates. A transversely isotropic thermoelastic nanoscale beam with two temperatures and with Green-Naghdi (GN) III theory of thermoelasticity for free vibrations with simply supported boundaries have been examined by Kaur *et al.* (2021).

The objective of this paper is to consider two dimensional transversely isotropic new modified couple stress generalized thermoelastic plate without energy dissipation and with two temperatures

due to axisymmetric heat supply. The solution is found by using Laplace and Hankel transform techniques. The analytical expressions of displacement components, stress components, conductive temperature and couple stress are computed in transformed domain. Numerical inversion technique has been applied to obtain the results in the physical domain. Numerically simulated results are depicted graphically. The effect of two temperature parameter is shown on the various components.

### 2. Basic equations

Following Chen and Li (2014), Youssef (2011) and Devi(), the field equations transversely isotropic thermoelastic medium using new modified couple stress theory in the absence of body forces, body couple and without energy dissipation and with two temperature are given by

$$t_{ij} = c_{ijkl}\epsilon_{kl} + \frac{1}{2}e_{ijk}m_{lk,l} - \beta_{ij}T, \tag{1}$$

$$c_{ijkl}e_{kl,j} + \frac{1}{2}e_{ijk}m_{lk,lj} - \beta_{ij}T_{,j} = \rho\dot{u}_i, \tag{2}$$

$$K_{ij}\varphi_{,ij} - \rho C_E \ddot{T} = \beta_{ij}T_0\ddot{\epsilon}_{ij}, \tag{3}$$

where

$$\beta_{ij} = c_{ijkl}\alpha_{ij}, \tag{4}$$

$$\epsilon_{ij} = \frac{1}{2}(u_{i,j} + u_{j,i}), \tag{5}$$

$$m_{ij} = l_i^2 G_i \chi_{ij} + l_j^2 G_j \chi_{ji}, \tag{6}$$

$$\chi_{ij} = \omega_{i,j}, \tag{7}$$

$$\omega_i = \frac{1}{2}e_{ijk}u_{k,j}, \tag{8}$$

$$T = \varphi - a_{ij}\varphi_{,ij}. \tag{9}$$

$T_0$  is assumed to be such that  $T/T_0 \ll 1$ , and  $\beta_1 = (c_{11} + c_{12})\alpha_1 + c_{13}\alpha_3$ ,  $\beta_3 = 2c_{13}\alpha_1 + c_{33}\alpha_3$ .

### 3. Formulation and solution of the problem

Consider a thick circular plate of thickness  $2d$  occupying the space  $D$  defined by  $0 \leq r \leq \infty, -d \leq z \leq d$ . Consider cylindrical polar coordinate system  $(r, \theta, z)$  with symmetry about  $z$ -axis. Cylindrical polar coordinates  $(r, \theta, z)$  having origin on the surface  $z=0$ , between the lower and upper surfaces of the plate and the  $z$ -axis normal to plate. The  $z$ -axis is assumed to be the axis of symmetry. The problem considered is plane axisymmetric,  $u_\theta = 0$ , and  $u_r, u_z$  and  $T$  are independent of  $\theta$  and are functions of  $(r, z, t)$ . The initial temperature in the plate is given a

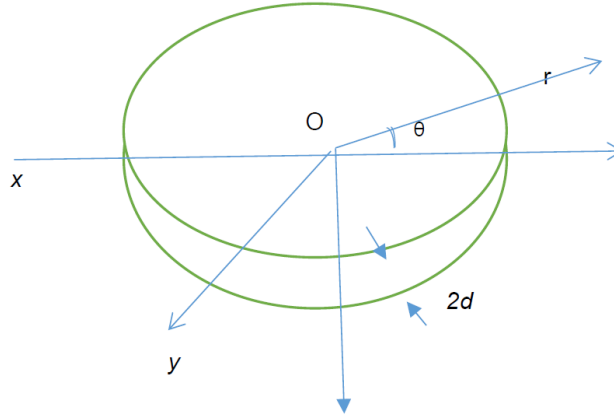


Fig. 1 Circular plate

constant temperature  $T_0$ , and the heat flux of magnitude  $g_0 F(r, z)$  is prescribed on the upper and lower boundary surfaces. For  $t > 0$ , heat is generated within the plate at a rate  $F(r, t)$ . We consider a normal surface (ring source) which emanates from the origin of the coordinate axis and expands radially at constant rate cover the surface. Under these conditions thermoelastic quantities due to the ring load are to be determined. As the problem considered is two dimensional.

$$\begin{aligned} u &= u(r, z, t), \\ w &= w(r, z, t), \\ \varphi &= \varphi(r, z, t). \end{aligned} \quad (10)$$

$$c_{11} \left( \frac{\partial^2 u}{\partial r^2} + \frac{\partial u}{r \partial r} - \frac{u}{r^2} \right) + c_{44} \frac{\partial^2 u}{\partial z^2} + (c_{13} + c_{44}) \frac{\partial^2 w}{\partial r \partial z} + \frac{1}{4} l_2^2 G_2 \left( \frac{\partial^4 u}{\partial r^2 \partial z^2} - \frac{\partial^4 w}{\partial r^3 \partial z} + \frac{\partial^4 u}{\partial z^4} - \frac{\partial^4 w}{\partial z^3 \partial r} \right) - \beta_1 \frac{\partial}{\partial r} \left( 1 - a_1 \left( \frac{\partial^2}{\partial r^2} + \frac{\partial}{r \partial r} \right) - a_3 \frac{\partial^2}{\partial z^2} \right) \varphi = \rho \ddot{u}, \quad (11)$$

$$c_{33} \frac{\partial^2 w}{\partial z^2} + (c_{44} + c_{13}) \left( \frac{\partial^2 u}{\partial r \partial z} + \frac{\partial u}{r \partial z} \right) + c_{44} \left( \frac{\partial^2 w}{\partial r^2} + \frac{\partial w}{r \partial r} \right) + \frac{1}{4} l_2^2 G_2 \left( \left( \frac{\partial^3}{\partial r^2 \partial z} + \frac{\partial^3}{\partial r^2 \partial z} \right) \left( \frac{\partial}{\partial r} + \frac{1}{r} \right) u - \left( \frac{\partial^3}{\partial r^3} + \frac{\partial^3}{\partial r \partial z^2} \right) \left( \frac{\partial}{\partial r} + \frac{1}{r} \right) w \right) - \beta_3 \frac{\partial}{\partial z} \left( 1 - a_1 \left( \frac{\partial^2}{\partial r^2} + \frac{\partial}{r \partial r} \right) - a_3 \frac{\partial^2}{\partial z^2} \right) \varphi = \rho \ddot{w}, \quad (12)$$

$$K_1 \left( \frac{\partial^2 \varphi}{\partial r^2} + \frac{\partial \varphi}{r \partial r} \right) + K_3 \frac{\partial^2 \varphi}{\partial z^2} - \rho c_E \frac{\partial^2}{\partial t^2} \left( 1 - a_1 \left( \frac{\partial^2}{\partial r^2} + \frac{\partial}{r \partial r} \right) - a_3 \frac{\partial^2}{\partial z^2} \right) \varphi = T_0 \frac{\partial^2}{\partial t^2} \left( \beta_1 \frac{\partial u}{\partial r} + \beta_3 \frac{\partial w}{\partial z} \right). \quad (13)$$

The constitutive equations and couple stress components are

$$\begin{aligned} t_{zz} &= c_{13} e_{rr} + c_{13} e_{\theta\theta} + c_{33} e_{zz} - \beta_3 T \\ t_{rz} &= 2c_{44} e_{rz} - \frac{1}{4} l_2^2 G_2 \left( \frac{\partial^3 u}{\partial z \partial r^2} + \frac{\partial^3 u}{\partial z^3} - \frac{\partial^3 w}{\partial r^3} - \frac{\partial^3 w}{\partial r \partial z^2} \right), \\ t_{\theta\theta} &= c_{21} e_{rr} + c_{11} e_{\theta\theta} + c_{13} e_{zz} - \beta_1 T, \\ t_{rr} &= c_{11} e_{rr} + c_{12} e_{\theta\theta} + c_{13} e_{zz} - \beta_1 T, \quad m_{\theta z} = \frac{1}{2} l_2^2 G_2 \left( \frac{\partial^2 u}{\partial z^2} - \frac{\partial^2 w}{\partial z \partial r} \right), \\ m_{r\theta} &= -\frac{1}{2} l_2^2 G_2 \left( \frac{\partial^2 u}{\partial z \partial r} - \frac{\partial^2 w}{\partial r^2} \right) \end{aligned} \quad (14)$$

where

$$e_{rr} = \frac{\partial u}{\partial r}, e_{rz} = \frac{1}{2} \left( \frac{\partial u}{\partial z} + \frac{\partial w}{\partial r} \right), e_{\theta\theta} = \frac{u}{r}, e_{zz} = \frac{\partial w}{\partial z},$$

$$T = \left( 1 - a_1 \left( \frac{\partial^2}{\partial r^2} + \frac{\partial}{r \partial r} \right) - a_3 \frac{\partial^2}{\partial z^2} \right) \varphi.$$

In the above equation we use contracting subscript notation (1 → 11, 2 → 22, 3 → 33, 4 → 23, 5 → 31, 6 → 12) to relate  $c_{ijkl}$  to  $c_{mn}$ .

To facilitate the solution, we define the dimensionless quantities are defined as

$$r' = \frac{r}{L}, z' = \frac{z}{L}, t' = \frac{c_1}{L} t, u' = \frac{\rho c_1^2}{L \beta_1 T_0} u, w' = \frac{\rho c_1^2}{L \beta_1 T_0} w, T' = \frac{T}{T_0}, \varphi' = \frac{\varphi}{T_0}, t'_{zr} = \frac{t_{zr}}{\beta_1 T_0} t'_{rr} = \frac{t'_{rr}}{\beta_1 T_0}, m'_{32} = \frac{m_{32}}{L \beta_1 T_0}, a_1' = \frac{a_1}{L^2}, a_3' = \frac{a_3}{L^2}, \rho c_1^2 = c_{11}. \tag{15}$$

Where  $L$  is constant of dimensions of length.

Defining Laplace and Hankel transformation as

$$\hat{f}(r, z, s) = \int_0^\infty f(r, z, t) e^{-st} dt, \tag{16}$$

$$\tilde{f}(\xi, z, s) = \int_0^\infty \hat{f}(r, z, s) r J_n(r\xi) dr. \tag{17}$$

Applying the dimensionless quantities defined by (15) and Laplace Hankel defined by (16)-(17) to the Eqs. (11)-(13), we obtain

$$\left( \delta_8 + \delta_2 D^2 - \frac{l_2^2 G_2}{4L^2 c_{11}} (D^4 - \xi^2 D^2) \right) \tilde{u} + (-\delta_1 \xi D + \frac{l_2^2 G_2}{4L^2 c_{11}} (-\xi^3 D + \xi D^3)) \tilde{w} + \xi (1 + a_1 \xi^2 - a_3 D^2) \tilde{\varphi} = 0, \tag{18}$$

$$(\delta_1 \delta_9 D - \frac{l_2^2 G_2}{4L^2 c_{11}} \delta_9 (-\xi^2 D + D^3)) \tilde{u} + (\delta_{10} + \delta_3 D^2 + \frac{l_2^2 G_2}{4L^2 c_{11}} (-\xi^3 + D^2) \delta_9) \tilde{w} - \frac{\beta_3}{\beta_1} D (1 + a_1 \xi^2 - a_3 D^2) \tilde{\varphi} = 0, \tag{19}$$

$$\delta_6 \xi s^2 \tilde{u} - \delta_7 D s^2 \tilde{w} + (\delta_{11} + (\delta_4 + \delta_5 s^2 a_3) D^2) \tilde{\varphi} = 0, \tag{20}$$

where

$$D = \frac{d}{dz}, \delta_1 = \frac{c_{13} + c_{44}}{c_{11}}, \delta_2 = \frac{c_{44}}{c_{11}}, \delta_3 = \frac{c_{33}}{c_{11}}, \delta_4 = \frac{K_3}{K_1}, \delta_5 = \frac{\rho c_E c_1^2}{K_1}, \delta_6 = \frac{T_0 \beta_1^2}{K_1 \rho}, \delta_7 = \frac{T_0 \beta_1 \beta_3}{K_1 \rho}, \delta_8 = -(s^2 + \xi^2), \delta_9 = \frac{-\xi^2 + 1}{\xi}, \delta_{10} = -\delta_2 \delta_9 - s^2, \delta_{11} = -\xi^2 - \delta_5 s^2 (1 + a_1 \xi^2).$$

The non trivial solution of the system of Eqs. (18)-(20) yields

$$(PD^8 + QD^6 + RD^4 + SD^2 + T)(\tilde{u}, \tilde{w}, \tilde{\varphi}) = 0, \tag{21}$$

Where

$$P = \delta_{12} \delta_{16} \delta_3 - \delta_{12} \delta_7 s^2 \delta_{12} a_3 - \delta_{12}^2 \delta_{11} \delta_3 \delta_9,$$

$$Q = \delta_{17} \delta_{16} \delta_3 + \delta_{17} \delta_7 \delta_{15} s^2 a_3 - \delta_{12} \delta_{11} \delta_{20} - \delta_{12} \delta_{16} \delta_{14} - \delta_{12} \delta_7 \delta_{15} s^2 (1 + a_1 \xi^2) + (-\delta_{18} + \delta_{12} \xi^3) \delta_{12} \delta_9 \delta_{16} - \xi a_3 \delta_{12} \delta_9 \delta_7 + \delta_{12} \delta_9 (\delta_1 \delta_9 \delta_{16} - \delta_{12} \delta_9 \delta_{11} - \delta_6 s^2 \xi a_3 \delta_{15}),$$

$$R = \delta_8 \delta_{16} \delta_3 + \delta_8 \delta_7 \delta_{15} s^2 a_3 + \delta_{20} \delta_{11} \delta_{17} + \delta_{17} \delta_{16} \delta_{14} - \delta_{17} \delta_7 \delta_{15} s^2 (1 + a_1 \xi^2) - \delta_{12} \delta_{11} \delta_{14} - (-\delta_{18} + \delta_{12} \xi^3) (\delta_{19} \delta_{16} - \delta_{12} \delta_9 \delta_{11} - \delta_6 s^2 \xi a_3 \delta_{15}) + \delta_{13} \delta_{12} \delta_9 s^2 + \xi a_3 \delta_1 \delta_9 \delta_7 s^2 + \xi a_3 \delta_6 s^2 \xi^2 + \delta_{12} \delta_9 \delta_{11} \xi^2 s^2 (1 + a_1 \xi^2),$$

$$S = \delta_8 \delta_{11} \delta_{20} + \delta_8 \delta_{16} \delta_{14} + \delta_8 \delta_7 s^2 \delta_{15} (1 + a_1 \xi^2) + \delta_{17} \delta_{11} \delta_{14} + (\delta_1 \delta_{11} \delta_9 + \delta_6 s^2 \xi \delta_{15}) (-\delta_{18} + \delta_{12} \xi^3) (1 + a_1 \xi^2) - \delta_{13} \delta_1 \delta_9 \delta_7 s^2 - \delta_6 \delta_{13} s^2 \xi + \delta_6 s^2 \xi^2 a_3 \delta_{14} + \delta_1 \delta_{11} \delta_9^2 \xi \delta_{12}$$

$$T = \delta_8 \delta_{11} \delta_{14} - \delta_{13} \delta_6 \delta_{14} s^2 \xi.$$

The roots of the Eq. (21) are  $\pm \lambda_i (i = 1, 2, 3, 4, 5)$ , using the radiation condition that  $\hat{u}, \hat{w}, \hat{\phi} \rightarrow 0$  as  $z \rightarrow \infty$  the solution of Eq. (20) may be written as

$$\tilde{u} = \sum_{i=1}^4 A_i \cosh(\lambda_i z), \quad (22)$$

$$\tilde{v} = \sum_{i=1}^4 R_i A_i \cosh(\lambda_i z), \quad (23)$$

$$\tilde{w} = \sum_{i=1}^4 S_i A_i \cosh(\lambda_i z), \quad (24)$$

Where

$$R_i = \frac{P^* \lambda_i^6 + Q^* \lambda_i^4 + R^* \lambda_i^2 + S^*}{A^* \lambda_i^4 + B^* \lambda_i^2 + C^*},$$

$$S_i = \frac{P^{**} \lambda_i^6 + Q^{**} \lambda_i^4 + R^{**} \lambda_i^2 + S^{**}}{A^* \lambda_i^4 + B^* \lambda_i^2 + C^*},$$

where

$$P^* = -\delta_{12} \delta_{16}, \quad Q^* = \delta_{17} \delta_{16} - \delta_{12} \delta_{11},$$

$$R^* = \delta_8 \delta_{16} - \delta_{17} \delta_{11} - \delta_6 s^2 \xi^2 a_3,$$

$$S^* = \delta_8 \delta_{11} - \delta_6 s^2 \xi \delta_{13}, \quad P^{**} = -\delta_{12}^2 \delta_3,$$

$$Q^{**} = \delta_{17} \delta_{20} - \delta_{12} \delta_{14} - \delta_{12} \delta_9 \delta_{18},$$

$$R^{**} = \delta_8 \delta_{20} + \delta_{17} \delta_{14} + \delta_{19} \delta_{18}, \quad S^{**} = \delta_8 \delta_{14},$$

$$A^* = \delta_{16} \delta_3 + \delta_7 s^2 \delta_{15} a_3,$$

$$B^* = \delta_{11} \delta_{20} + \delta_{16} \delta_{14} - \delta_7 s^2 \delta_{15} (1 + a_1 \xi^2), \quad C^* = \delta_{11} \delta_{14}$$

$$\delta_{12} = \frac{l_2^2 G_2}{4L^2 c_{11}}, \delta_{13} = \beta_1 \xi (1 + a_1 \xi^2), \delta_{14} = \delta_{10} + \delta_{12} \delta_9 \xi^3, \delta_{15} = \frac{\beta_3}{\beta_1}, \delta_{16} = \delta_4 + \delta_5 s^2 a_3, \delta_{17} =$$

$$\delta_2 - \xi^2, \delta_{18} = -\delta_1 \xi - \delta_{12} \xi^3, \delta_{19} = \delta_1 \delta_9 + \delta_{12} \xi^2 \delta_9, \delta_{20} = \delta_3 + \delta_{12} \delta_9,$$

#### 4. Boundary conditions

$$\frac{\partial \phi}{\partial z} = \pm g_0 F(r, z), \text{ at } z = \pm d, \quad (25)$$

$$t_{zz} = f(r, t) \text{ at } z = \pm d, \quad (26)$$

$$t_{rz} = 0 \text{ at } z = \pm d, \quad (27)$$

$$m_{z\theta} = 0 \text{ at } z = \pm d, \quad (28)$$

The function  $F(r, z)$  considered in the problem falls off exponentially as one moves away from the centre of the plate in the radial direction and increases symmetrically along the axial direction given by

$$F(r, z) = z^2 e^{-\omega r}, \omega > 0, \quad (29)$$

$$f(r, t) = \frac{1}{2\pi r} \delta(ct - r). \quad (30)$$

and  $\delta(\cdot)$  is Dirac delta function

Applying Laplace and Hankel transform defined by (16)-(17) on (29) and (30) we get

$$\tilde{F}(\xi, z) = \frac{z^2 \omega}{(\xi^2 + \omega^2)^{3/2}}, \tag{31}$$

$$\tilde{f}(\xi, s) = \frac{1}{2\pi(\xi^2 + \frac{s^2}{c^2})^{1/2}}. \tag{32}$$

Substituting the  $u, w, \varphi$  from (22)-(24) and  $t_{zz}, t_{zr}, m_{z\theta}$  from (14) with the aid of (15) in the boundary conditions (27)-(30) and with the aid of (16)-(17) and (31)-(32), we obtain the expressions for displacement components, stress components, conductive temperature, and couple stress components are given in the appendix A.

### 5. Inversion of the transformations

To obtain the solution of the problem in physical domain, we must invert the transforms in Eqs. (A.1)-(A.9). Here the distance components, normal and tangential stresses, conductive temperature and couple stress are functions of  $z$ , the parameters of Hankel and laplace transforms are  $\xi$  and  $s$  respectively and hence are of the form  $\tilde{f}(\xi, z, s)$ . To obtain the function  $f(r, z, t)$  in the physical domain, we first invert the Hankel transform using

$$\hat{f}(r, z, s) = \int_0^\infty \xi \tilde{f}(\xi, z, s) J_n(\xi r) d\xi. \tag{33}$$

Now for the fixed values of  $\xi, r$  and  $z$  the function  $\hat{f}(r, z, s)$  in the expression above can be considered as the Laplace transform  $\hat{g}(s)$  of  $g(t)$ . Following Honig and Hirdes (1984), the Laplace transform function  $\hat{g}(s)$  can be inverted. The function  $g(t)$  can be obtained by using

$$g(t) = \frac{1}{2\pi i} \int_{C+i\infty}^{C-i\infty} e^{st} \hat{g}(s) ds, \tag{34}$$

where  $C$  is an arbitrary real number greater than all the real parts of the singularities of  $\hat{g}(s)$ . Taking  $s = C + iy$  we get

$$g(t) = \frac{e^{Ct}}{2\pi} \int_{-\infty}^\infty e^{ity} \hat{g}(C + iy) dy, \tag{35}$$

Now, taking  $e^{-Ct} g(t)$  as  $h(t)$  and expanding it as Fourier series in  $[0, 2L]$ , we obtain approximately the formula

$$g(t) = g_\infty(t) + E_D,$$

where

$$g_\infty(t) = \frac{C_0}{2} + \sum_{K=1}^\infty C_K, \quad 0 \leq t \leq 2L,$$

and

$$C_k = \frac{e^{Ct}}{L} \operatorname{Re} \left[ e^{\frac{\pi i k t}{L}} \hat{g} \left( C + \frac{i k \pi t}{L} \right) \right]. \tag{36}$$

$E_D$  is the discretization error and can be made arbitrarily small by choosing  $C$  large enough.

The value of  $C$  and  $L$  are chosen according to the criteria outlined by Honig and Hirdes (1984). Since the infinite series in (42) can be summed up only to a finite number of  $N$  terms, so the approximate value of  $g(t)$  becomes

$$g_N(t) = \frac{C_0}{2} + \sum_{K=1}^N C_K, \quad 0 \leq t \leq 2L. \tag{37}$$

Now, we introduce a truncation error  $E_T$ , that must be added to the discretization error to produce the total approximate error in evaluating  $g(t)$  using the above formula. To accelerate the convergence, the discretization error and then the truncation error is reduced by using the 'Korrektur method' and the ' $\epsilon$ -algorithm', respectively as given by Honig and Hirdes (1984).

The Korrektur method formula, to evaluate the function  $g(t)$  is

$$g(t) = g_\infty(t) - e^{-2CL} g_\infty(2L + t) + E'_D,$$

where

$$|E'_D| \ll |E_D|.$$

Thus, the approximate value of  $g(t)$  becomes

$$g_{Nk}(t) = g_N(t) - e^{-2CL} g_{N'}(2L + t), \quad (38)$$

where  $N'$  is an interger such that  $N' < N$ .

We shall now describe the  $\epsilon$ -algorithm, which is used to accelerate the convergence of the series in (37). Let  $N$  be an odd natural number and  $S_m = \sum_{k=1}^m C_k$  be the sequence of partial sums of (37). we define the ' $\epsilon$ -sequence' by

$$\epsilon_{0,m} = 0, \epsilon_{1,m} = S_m, \epsilon_{n+1,m} = \epsilon_{n-1,m+1} \frac{1}{\epsilon_{n,m+1} - \epsilon_{n,m}}; n, m = 1, 2, 3 \dots \dots$$

The sequence  $\epsilon_{1,1}, \epsilon_{3,1}, \dots \dots \epsilon_{N,1}$  converges to  $g(t) + E_D - \frac{C_0}{2}$  faster than the sequence of partial sums  $S_m$ ,  $m = 1, 2, 3, \dots \dots$ . The actual procedure to invert the Laplace transform consists of (38) together with the ' $\epsilon$ -algorithm'.

The last step is to calculate the integral in Eq. (33). The method for evaluating this integral is described in Press *et al.* (1986). It involves the use of Romberg's integration with adaptive step size. This also uses the results from successive refinements of the extended trapezoidal rule followed by extrapolation of the results to the limit when the step size tends to zero.

## 6. Results and discussions

Even though copper is face centered cubic it has significant mechanical anisotropy depending on the crystallographic orientations. For numerical computations, following Lata (2015), we take the copper material as

$$\begin{aligned} c_{11} &= 18.78 \times 10^{10} \text{ Kgm}^{-1}\text{s}^{-2}, \\ c_{12} &= 8.76 \times 10^{10} \text{ Kgm}^{-1}\text{s}^{-2}, \\ c_{13} &= 8.0 \times 10^{10} \text{ Kgm}^{-1}\text{s}^{-2}, \\ c_{33} &= 17.2 \times 10^{10} \text{ Kgm}^{-1}\text{s}^{-2}, \\ c_{44} &= 5.06 \times 10^{10} \text{ Kgm}^{-1}\text{s}^{-2}, \\ C_E &= 0.6331 \times 10^3 \text{ JKg}^{-1}\text{K}^{-1}, \\ \alpha_1 &= 2.98 \times 10^{-5} \text{ K}^{-1}, \\ \alpha_3 &= 2.4 \times 10^{-5} \text{ K}^{-1}, \\ T_0 &= 293 \text{ K}, \\ \rho &= 8.954 \times 10^3 \text{ Kgm}^{-3}, \\ T_0 &= 293 \text{ K}, \\ \rho &= 8.954 \times 10^3 \text{ Kgm}^{-3}, \\ K_1 &= 0.433 \times 10^3 \text{ Wm}^{-1}\text{K}^{-1}, \end{aligned}$$

$$\begin{aligned}
 K_3 &= 0.450 \times 10^3 \text{Wm}^{-1}\text{K}^{-1}, \\
 G_1 &= 0.1, \quad G_2 = 0.2, \quad G_3 = 0.3, \\
 l_1 &= l_2 = l_3 = .2 \text{ nm} \\
 t &= .01\text{s} \quad L = 1
 \end{aligned}$$

The values of displacement components  $u$  and  $w$ , conductive temperature  $\phi$ , stress components  $t_{rr}, t_{\theta\theta}, t_{zz}$  and  $t_{zr}$ , and couple stress components  $m_{z\theta}$  and  $m_{r\theta}$ , w.r.t. $r$  and w.r.t. $z$ , without energy dissipation and with two temperatures are presented graphically to show the influence of two temperature parameter.

- i) The solid line in black with central symbol square corresponds to  $a_1 = a_3 = 0$ .
- ii) The solid line in red with central symbol circle corresponds to  $a_1 = a_3 = .07$ .

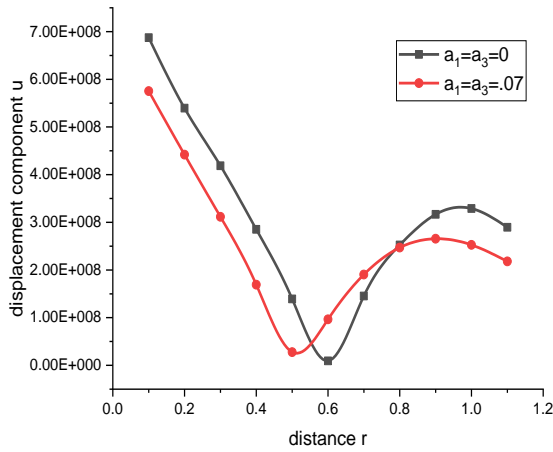


Fig. 2 Variation of displacement component  $u$  with the distance  $r$

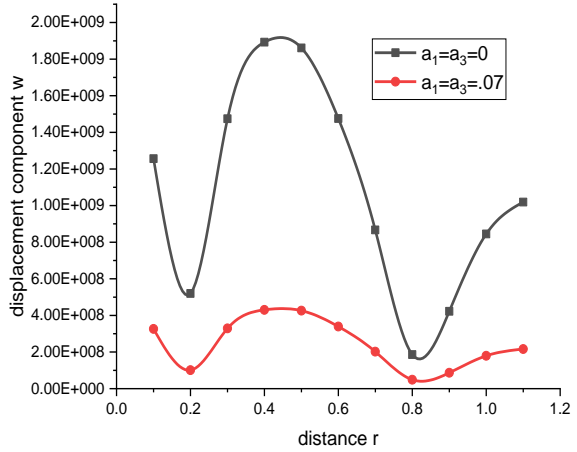


Fig. 3 Variation of displacement component  $w$  with the distance  $r$

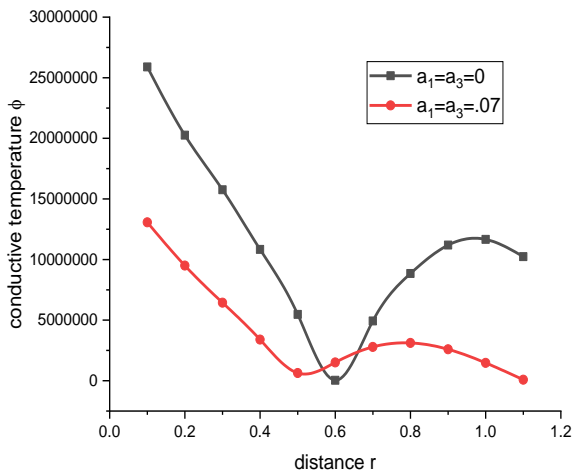


Fig. 4 Variation of conductive temperature  $\phi$  with the distance  $r$

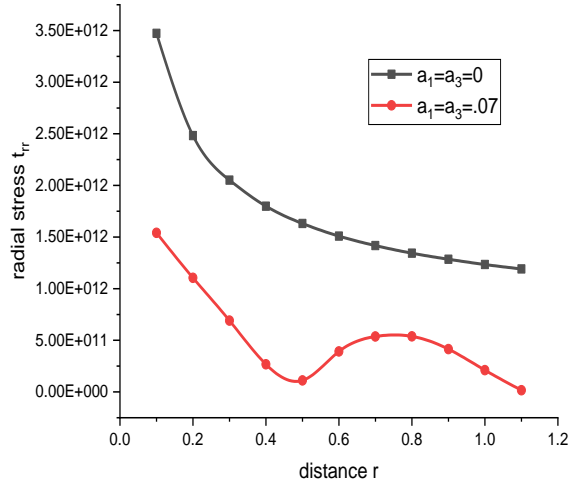


Fig. 5 Variation of radial stress  $t_{rr}$  with the distance  $r$

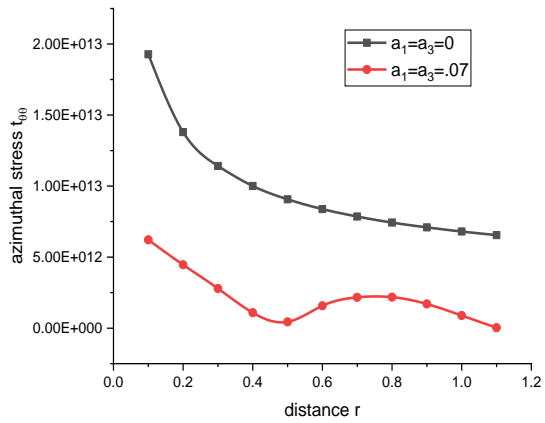


Fig. 6 Variation of azimuthal stress  $t_{\theta\theta}$  with the distance  $r$

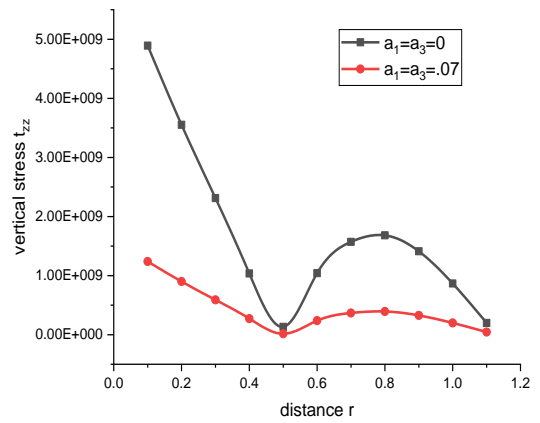


Fig. 7 Variation of vertical stress  $t_{zz}$  with the distance  $r$

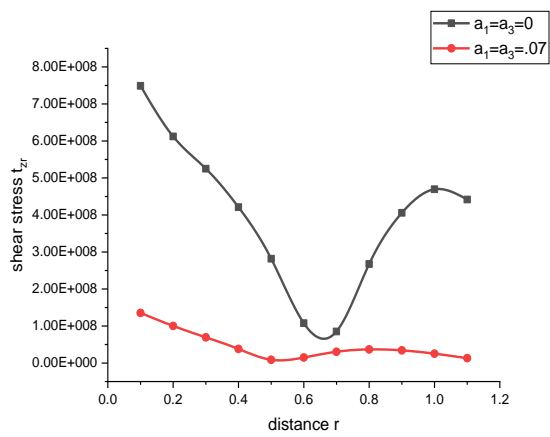


Fig. 8 Variation of shear stress  $t_{zr}$  with the distance  $r$

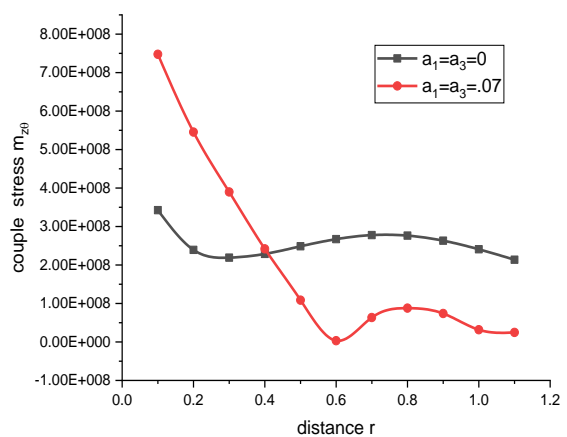


Fig. 9 Variation of couple stress  $m_{z\theta}$  with the distance  $r$

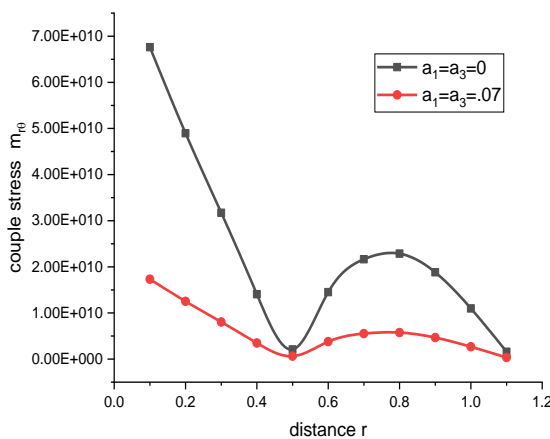


Fig. 10 Variation of couple stress  $m_{r\theta}$  with the distance  $r$

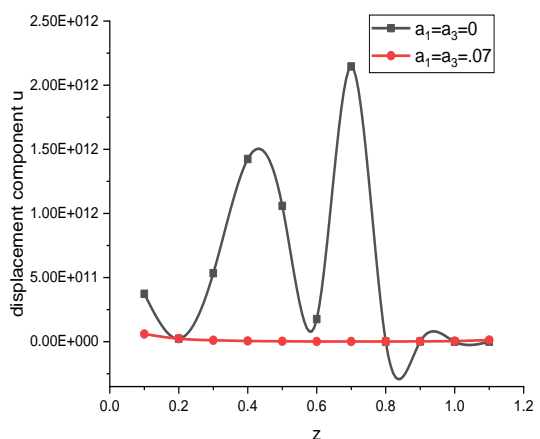


Fig. 11 Variation of displacement component  $u$  with the  $z$  coordinate

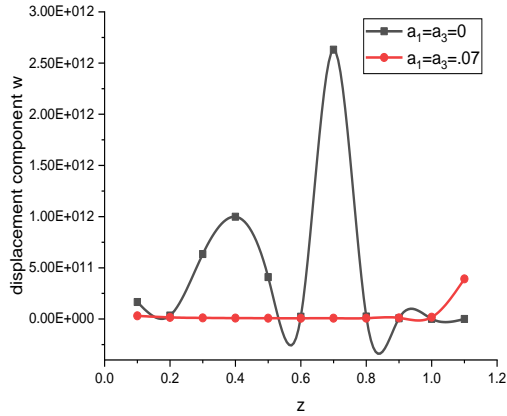


Fig. 12 Variation of displacement component  $w$  with the  $z$  coordinate

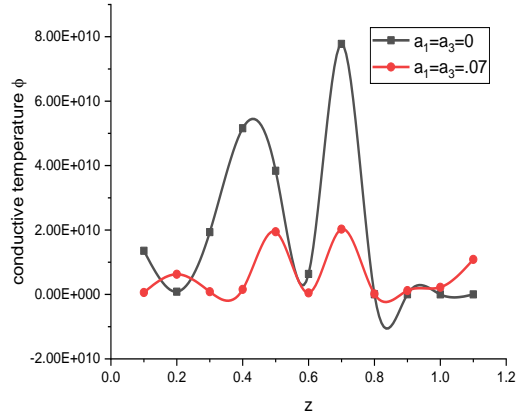


Fig. 13 Variation of conductive temperature  $\phi$  with the  $z$  coordinate

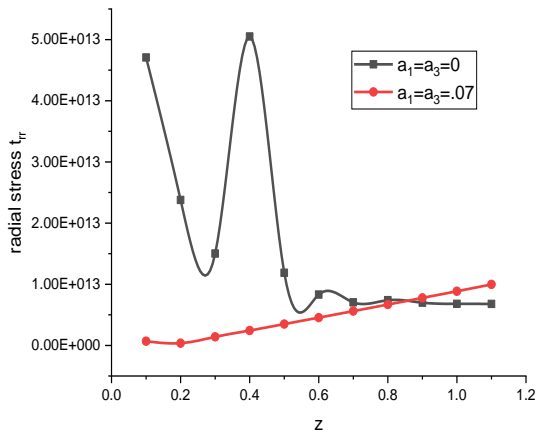


Fig. 14 Variation of radial stress  $t_{rr}$  with the  $z$  coordinate

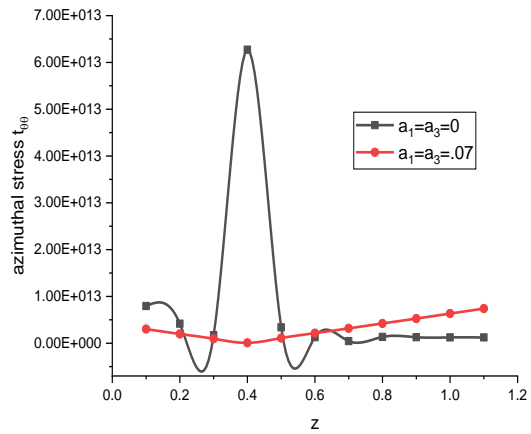


Fig. 15 Variation of azimuthal stress  $t_{\theta\theta}$  with the  $z$  coordinate

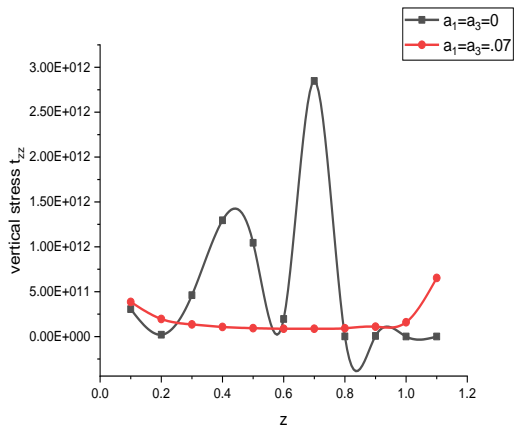


Fig. 16 Variation of vertical stress  $t_{zz}$  with the  $z$  coordinate

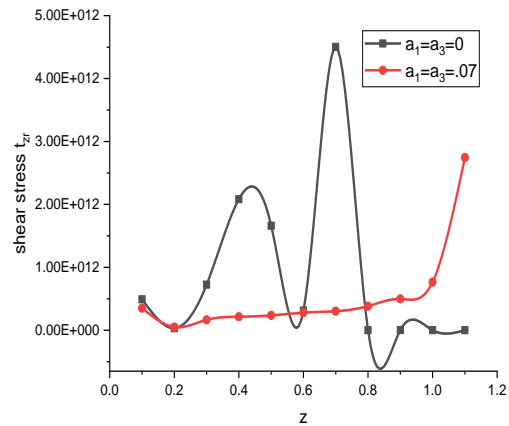


Fig. 17 Variation of shear stress  $t_{zr}$  with the  $z$  coordinate

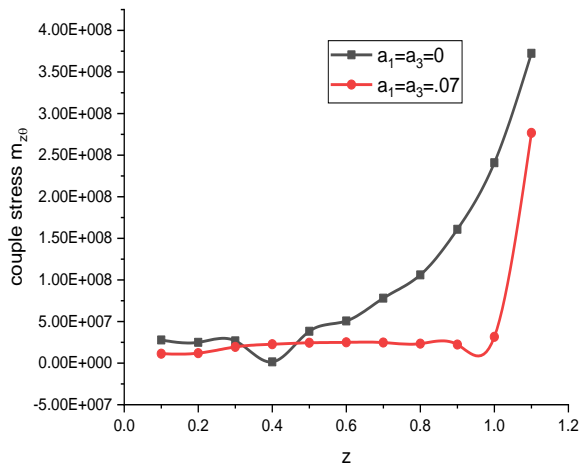


Fig. 18 Variation of couple stress  $m_{z\theta}$  with the z coordinate

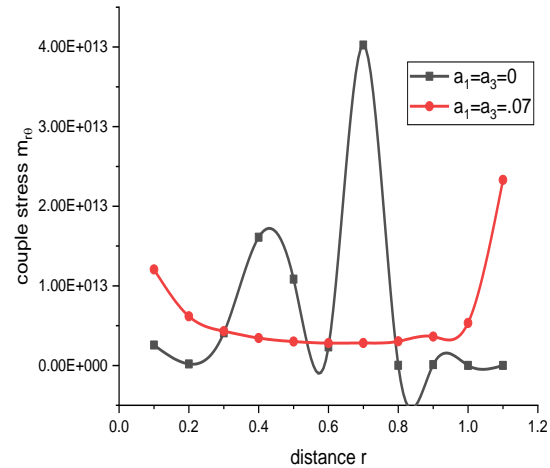


Fig. 19 Variation of couple stress  $m_{r\theta}$  with the z coordinate

*For variation w.r.t r*

In Fig. 2 displacement component u follow decreases in the first half range, increases in  $0.55 \leq r \leq 1$  and then decreases. In Fig. 3 displacement component w follow oscillatory trend. Inclusion of two temperature parameter decreases the amplitude of oscillations. In Fig. 4 conductive temperature  $\varphi$  follows similar pattern as that of displacement component u. In Fig. 5 radial stress  $t_{rr}$  and in Fig. 6 azimuthal stress  $t_{\theta\theta}$  decrease for  $a_1 = a_3 = 0$  with the increase of r. for  $a_1 = a_3 = .07$   $t_{rr}$  and  $t_{\theta\theta}$  follow consecutively decreasing increasing pattern. In Fig. 7 vertical stress  $t_{zz}$  follows similar pattern as that of displacement u except the magnitude In Fig. 8 shear stress  $t_{zr}$  decreases in the first half range and increases in remaining range. For given r inclusion of two temperature decreases the magnitude of variation. In Fig. 9 couple stress  $m_{z\theta}$  is oscillatory in pattern. In Fig. 10  $m_{r\theta}$  decreases for  $0.1 \leq r \leq 0.5$ , increases in  $0.5 \leq r \leq 1$ , and decreases again in the remaining range.

*For variation w.r.t z*

In Fig. 11 displacement component u for  $a_1 = a_3 = 0$  follows oscillatory pattern w.r.t.z. For  $a_1 = a_3 = .07$  sketch is almost linear. In Fig. 12 displacement component w for  $a_1 = a_3 = 0$  follows oscillatory pattern w.r.t.z. For  $a_1 = a_3 = .07$  sketch is linear for  $0.1 \leq r \leq 1$  and increases a little in the remaining range w.r.t.z. In Fig. 13 conductive temperature  $\varphi$  pursues oscillatory pattern. Inclusion of two temperature parameter decreases the distance between consecutive crests and troughs. In Figs. 14-15 variations for radial stress, azimuthal stress are oscillatory for  $a_1 = a_3 = 0$ . For  $a_1 = a_3 = .07$  value of physical quantities increases with the increase in z. In Fig. 16 vertical stress is oscillatory for  $a_1 = a_3 = 0$ . For  $a_1 = a_3 = .07$  sketch is curvilinear. In Fig. 17 variation for shear stress  $t_{zr}$  is oscillatory for  $a_1 = a_3 = 0$ . For  $a_1 = a_3 = .07$  sketch decreases w.r.t.z initially the increases w.r.t.z. In Fig. 18 for  $m_{z\theta}$  variation do not follow a proper pattern. In Fig. 19 variation for couple stress  $m_{r\theta}$  is similar to corresponding variation for radial stress  $t_{rr}$ .

## 7. Conclusions

Analysis of displacement components, stresses, conductive temperature cut these words due to ring load in a thick circular plate is a significant problem of continuum mechanics. The result obtained from above study are summarized as.

The resulting quantities depicted graphically are observed to be very sensitive towards the two temperature parameter. Figures show that the two-temperature parameter changes the magnitude the physical quantities obtained after computational process. It is also observed that the physical quantities in the absence of two temperature parameters are oscillatory for variation w.r.t.  $z$ . Presence of two temperature parameter changes variation from oscillatory to curvilinear. The results obtained in the study should be beneficial for people working on transversely isotropic new modified couple stress thermoelastic solid with mass diffusion. By introducing the two temperature parameter to the assumed model present a more realistic mode for future study.

## References

- Chen, D., Feng, K. and Zheng, S. (2019), "Flapwise vibration analysis of rotating composite laminated Timoshenko microbeams with geometric imperfection based on a re-modified couple stress theory and isogeometric analysis", *Eur. J. Mech. A/Solid.*, **76**, 25-35. <https://doi.org/10.1016/j.euromechsol.2019.03.002>.
- Chen, W. and Li, X. (2013), "Size-dependent free vibration analysis of composite laminated Timoshenko beam based on new modified couple stress theory", *Arch. Appl. Mech.*, **83**, 431-444. <https://doi.org/10.1007/s00419-012-0689-2>.
- Chen, W. and Si, J. (2013), "A model of composite laminated beam based on the global-local theory and new modified couple-stress theory", *Compos. Struct.*, **103**, 99-107. <https://doi.org/10.1016/j.compstruct.2013.03.021>.
- Chen, W. and Wang, Y. (2016), "A model of composite laminated Reddy plate of the global-local theory based on new modified couple-stress theory", *Mech. Adv. Mater. Struct.*, **23**(6), 636-651. <https://doi.org/10.1080/15376494.2015.1028691>.
- He, D., Yang, W. and Chen, W. (2017), "A size-dependent composite laminated skew plate model based on a new modified couple stress theory", *Acta Mechanica Solida Sinica*, **30**(1), 75-86. <https://doi.org/10.1016/j.camss.2016.12.001>.
- Honig, G. and Hirdes, U. (1984), "A method for the numerical inversion of the Laplace transform", *J. Comput. Appl. Math.*, **10**(1), 113-132. [https://doi.org/10.1016/0377-0427\(84\)90075-X](https://doi.org/10.1016/0377-0427(84)90075-X).
- Li, L., Chen, W.J. and Nan, Z. (2013), "Model of composite laminated thin plate based on modified couple stress theory and buckling analysis of scale effects", *Eng. Mech.*, **30**(5), 1-7. <http://doi.org/10.6052/j.issn.1000-4750.2011.11.0750>.
- Mazur, O., Kurpa, L. and Awrejcewicz, J. (2020), "Vibrations and buckling of orthotropic small-scale plates with complex shape based on modified couple stress theory", *Zeitschrift für Angewandte Mathematik und Mechanik*, **100**(1), e202000009. <http://doi.org/10.1002/zamm.202000009>.
- Press, W.H., Teukolsky, S.A., Vetterling, W.T. and Flannery, B.P. (1986), *Numerical Recipe*, Cambridge University Press.
- Si, J., Zhang, Y. and Yin, D. (2022), "Thermal scale effect analysis of enhanced Reddy's laminated composite based on new modified couple stress theory", *Acta Materiae Compositae Sinica*, **39**(1), 424-430. <http://doi.org/10.13801/j.cnki.fhclxb.20210301.003>.
- Yang, S. and Chen, W. (2015), "On hypotheses of composite laminated plates based on new modified couple stress theory", *Compos. Struct.*, **133**, 46-53. <https://doi.org/10.1016/j.compstruct.2015.07.050>.
- Yang, Z. and He, D. (2017), "Vibration and buckling of orthotropic functionally graded micro-plates on the

- basis of a re-modified couple stress theory”, *Results Phys.*, **7**, 3778-3787. <https://doi.org/10.1016/j.rinp.2017.09.026>.
- Yang, Z. and He, D. (2019), “A microstructure-dependent plate model for orthotropic functionally graded micro-plates”, *Mech. Adv. Mater. Struct.*, **26**(14), 1218-1225. <https://doi.org/10.1080/15376494.2018.1432794>.
- Yang, Z. and He, D. (2019), “Vibration and buckling of functionally graded sandwich micro-plates based on a new size-dependent model”, *Int. J. Appl. Mech.*, **11**(01), 1950004. <https://doi.org/10.1142/S1758825119500042>.
- Youssef, H.M. (2011), “Theory of two-temperature thermoelasticity without energy dissipation”, *J. Therm. Stress.*, **34**, 138-146. <https://doi.org/10.1080/01495739.2010.511941>.
- Zhang, R., Bai, H. and Chen, X. (2022), “The consistent couple stress theory-based vibration and post-buckling analysis of bi-directional functionally graded microbeam”, *Symmetry*, **14**, 602. <https://doi.org/10.3390/sym14030602>.
- Zhou, S., Zhang, R., Li, A., Qiao, J. and Zhou, S. (2022), “Analysis of transversely isotropic piezoelectric bilayered rectangular micro-plate based on couple stress piezoelectric theory”, *Eur. J. Mech. A/Solid.*, **96**, 104707. <https://doi.org/10.1016/j.euromechsol.2022.104707>.

AI

## Notation

$\mathbf{u} = (u, v, w)$	displacement vector
$c_{ijkl} (c_{ijkl} = c_{ijlk} = c_{jikl} = c_{jilk})$	Elastic parameters
$t_{ij}$	stress tensor
$e_{ij}$	Strain tensor
$\alpha_{ij}$	coefficients of linear thermal expansion
$\beta_{ij}$	thermal tensor
$T$	thermodynamical temperature
$\varphi$	conductive temperature
$l_i (i = 1, 2, 3)$	material length scale parameters
$\chi_{ij}$	Curvature
$\omega_i$	rotational vector
$\rho$	density of material
$K_{ij}$	materialistic constant
$c_E$	specific heat at constant strain
$T_0$	reference temperature
$G_i$	Elasticity constants
$m_{ij}$	Couple stress tensor
$a_{ij}$	Coefficients of two-temperature parameter tensor

**Appendix A**

$$\tilde{u} = \frac{g_0 \tilde{F}(\xi, d)}{\Delta} \sum_{i=1}^2 B_{1i} \cosh(\lambda_i z) + \frac{\tilde{f}(\xi, s)}{\Delta} \sum_{i=1}^2 B_{2i} \cosh(\lambda_i z), \tag{A.1}$$

$$\tilde{w} = \frac{g_0 \tilde{F}(\xi, d)}{\Delta} \sum_{i=1}^2 B_{1i} R_i \cosh(\lambda_i z) + \frac{\tilde{f}(\xi, s)}{\Delta} \sum_{i=1}^2 B_{2i} R_i \cosh(\lambda_i z), \tag{A.2}$$

$$\tilde{\phi} = \frac{g_0 \tilde{F}(\xi, d)}{\Delta} \sum_{i=1}^2 B_{1i} S_i \cosh(\lambda_i z) + \frac{\tilde{f}(\xi, s)}{\Delta} \sum_{i=1}^2 B_{2i} S_i \cosh(\lambda_i z), \tag{A.3}$$

$$\begin{aligned} \tilde{t}_{rr} = \frac{1}{\Delta} \sum_{i=1}^4 (g_0 \tilde{F}(\xi, d) B_{1i} + \tilde{f}(\xi, s) B_{2i}) & \left( \left( \left( \frac{c_{12}}{c_{11}} \frac{1}{\xi} - \xi \right) - (1 + a_1 \xi^2 - \right. \right. \\ & \left. \left. a_3 \lambda_i^2) S_i \right) \cosh(\lambda_i z) + \frac{c_{13}}{c_{11}} \lambda_i R_i \sinh(\lambda_i z) \right) \end{aligned} \tag{A.4}$$

$$\begin{aligned} \tilde{t}_{\theta\theta} = \frac{1}{\Delta} \sum_{i=1}^4 (g_0 \tilde{F}(\xi, d) B_{1i} + \tilde{f}(\xi, s) B_{2i}) & \left( \left( \left( -\frac{c_{12}}{c_{11}} \xi + \frac{1}{\xi} \right) - (1 + a_1 \xi^2 - \right. \right. \\ & \left. \left. a_3 \lambda_i^2) S_i \right) \cosh(\lambda_i z) + \frac{c_{13}}{c_{11}} \lambda_i R_i \sinh(\lambda_i z) \right) \end{aligned} \tag{A.5}$$

$$\begin{aligned} \tilde{t}_{zz} = \frac{g_0 \tilde{F}(\xi, d)}{\Delta} (\sum_{i=1}^4 \eta_i B_{1i} \cosh(\lambda_i z) + \sum_{i=1}^4 \mu_i B_{1i} \sinh(\lambda_i z)) + \\ \frac{\tilde{f}(\xi, s)}{\Delta} (\sum_{i=1}^4 \eta_i B_{2i} \cosh(\lambda_i z) + \sum_{i=1}^4 \mu_i B_{2i} \sinh(\lambda_i z)), \end{aligned} \tag{A.6}$$

$$\begin{aligned} \tilde{t}_{zr} = \frac{g_0 \tilde{F}(\xi, d)}{\Delta} (\sum_{i=1}^4 \nu_i B_{1i} \cosh(\lambda_i z) + \sum_{i=1}^4 \kappa_i B_{1i} \sinh(\lambda_i z)) + \\ \frac{\tilde{f}(\xi, s)}{\Delta} (\sum_{i=1}^4 \nu_i B_{2i} \cosh(\lambda_i z) + \sum_{i=1}^4 \kappa_i B_{2i} \sinh(\lambda_i z)), \end{aligned} \tag{A.7}$$

$$\begin{aligned} \tilde{m}_{\theta z} = \frac{g_0 \tilde{F}(\xi, d)}{\Delta} (\sum_{i=1}^4 \tau_i B_{1i} \cosh(\lambda_i z) + \sum_{i=1}^4 \chi_i B_{1i} \sinh(\lambda_i z)) + \\ \frac{\tilde{f}(\xi, s)}{\Delta} (\sum_{i=1}^4 \tau_i B_{2i} \cosh(\lambda_i z) + \sum_{i=1}^4 \chi_i B_{2i} \sinh(\lambda_i z)), \end{aligned} \tag{A.8}$$

$$\tilde{m}_{\theta r} = -\frac{1}{2} \frac{\beta_1 T_0}{L^2 \rho c_1^2} l_2^2 G_2 \sum_{i=1}^4 (\xi \lambda_i \sinh(\lambda_i z) + \xi^2 R_i \cosh(\lambda_i z)) (g_0 \tilde{F}(\xi, d) B_{1i} + \tilde{f}(\xi, s) B_{2i}) \tag{A.9}$$

where

$$\begin{aligned} \eta_i &= -\frac{c_{13}}{c_{11}} \xi - \frac{\beta_3}{\beta_1} \left( (1 + a_1 \xi^2) S_i - a_3 \lambda_i^2 S_i \right) \\ \mu_i &= \frac{c_{33}}{c_{11}} \lambda_i R_i \\ \kappa_i &= \frac{c_{44}}{c_{11}} \lambda_i - \frac{1}{4} \frac{\beta_1 T_0}{L^3 \rho c_1^2} l_2^2 G_2 (-\xi^2 \lambda_i + \lambda_i^3) \\ \nu_i &= -\xi R_i - \frac{1}{4} \frac{\beta_1 T_0}{L^3 \rho c_1^2} l_2^2 G_2 (-\xi^3 - \lambda_i^2 \xi) R_i \end{aligned}$$

$$\begin{aligned} \tau_i &= \frac{1}{2} \frac{\beta_1 T_0}{L^2 \rho c_1^2} l_2^2 G_2 \lambda_i^2 \\ \chi_i &= -\frac{1}{2} \frac{\beta_1 T_0}{L^2 \rho c_1^2} l_2^2 G_2 \xi \lambda_i R_i \\ A_{1i} &= \lambda_i S_i \sinh(\lambda_i d), \\ A_{2i} &= \eta_i \cosh(\lambda_i d) + \mu_i \sinh(\lambda_i d) \\ A_{3i} &= \kappa_i \sinh(\lambda_i d) + \nu_i \cosh(\lambda_i d), \\ A_{4i} &= \tau_i \cosh(\lambda_i d) + \chi_i \sinh(\lambda_i d) \quad i = 1, 2, 3, 4 \\ \Delta &= \Delta_1 - \Delta_2 + \Delta_3 - \Delta_4, \\ \Delta_1 &= A_{11} A_{22} (A_{33} A_{44} - A_{43} A_{34}) - A_{11} A_{23} (A_{32} A_{44} - A_{42} A_{34}) + A_{11} A_{24} (A_{32} A_{43} - A_{42} A_{33}), \\ \Delta_2 &= A_{12} A_{21} (A_{33} A_{44} - A_{43} A_{34}) - A_{12} A_{23} (A_{31} A_{44} - A_{41} A_{34}) + A_{24} A_{12} (A_{31} A_{43} - A_{41} A_{33}), \\ \Delta_3 &= A_{13} A_{21} (A_{32} A_{44} - A_{42} A_{34}) - A_{22} A_{13} (A_{31} A_{44} - A_{41} A_{34}) + A_{13} A_{24} (A_{31} A_{42} - A_{41} A_{32}), \\ \Delta_4 &= A_{14} A_{21} (A_{32} A_{43} - A_{42} A_{33}) - A_{22} A_{14} (A_{31} A_{43} - A_{41} A_{33}) + A_{14} A_{23} (A_{31} A_{42} - A_{41} A_{32}) \\ B_{1i} &= (-1)^{1+i} \Delta_i / A_{1i}, \\ B_{21} &= -A_{21} (A_{33} A_{44} - A_{43} A_{34}) + A_{23} (A_{31} A_{44} - A_{41} A_{34}) - A_{24} (A_{31} A_{43} - A_{41} A_{33}), \\ B_{22} &= A_{11} (A_{33} A_{44} - A_{43} A_{34}) - A_{13} (A_{31} A_{44} - A_{41} A_{34}) + A_{14} (A_{31} A_{43} - A_{41} A_{33}), \\ B_{23} &= -A_{11} (A_{23} A_{44} - A_{43} A_{24}) + A_{13} (A_{21} A_{44} - A_{41} A_{24}) - A_{14} (A_{21} A_{43} - A_{41} A_{23}), \\ B_{24} &= A_{11} (A_{23} A_{34} - A_{33} A_{24}) - A_{13} (A_{21} A_{34} - A_{31} A_{24}) + A_{14} (A_{21} A_{33} - A_{31} A_{23}). \end{aligned}$$